EPJ Web of Conferences **175**, 13006 (2018) https://doi.org/10.1051/epjconf/201817513006
Lattice 2017

Inclusive B decay calculations with analytic continuation

Shoji Hashimoto[1,2,⋆], *Brian* Colquhoun[1], *Taku* Izubuchi[3], *Takashi* Kaneko[1,2], and *Hiroshi* Ohki[4]

[1] *High Energy Accelerator Research Organization (KEK), Tsukuba 305-0801, Japan*
[2] *SOKENDAI (Graduate University for Advanced Studies), Tsukuba 305-0801, Japan*
[3] *Brookhaven National Laboratory, Upton, NY, 11973, USA*
[4] *Department of Physics, Nara Women's University, Nara 630-8506, Japan*

Abstract. First-principle lattice calculation of inclusive B meson semileptonic decays is possible for a certain class of moments that is connected to the structure function at unphysical kinematics by analytic continuation. We present an exploratory lattice calculation and a comparison with the heavy quark expansion technique.

1 Introduction

There is a long-standing tension in the determination of the Kobayashi-Maskawa matrix elements $|V_{cb}|$ and $|V_{ub}|$ between the exclusive and inclusive methods. (For a recent review, see [1].) For instance, the inclusive determination of $|V_{cb}|$ from the quark-level $b \to c\ell\nu$ is larger than that determined with the exclusive mode $B \to D^*\ell\nu$ by about two standard deviations. The exclusive determination uses the lattice inputs for the (zero-recoil) form factor for the corresponding decay modes, while the inclusive determination uses the *continuum* techniques, *i.e.* perturbative QCD and heavy quark expansion. In this talk, we try to formulate a method to use the lattice calculation for the inclusive decays.

The best known example of the inclusive analysis in QCD is the perturbative calculation of the R-ratio for the e^+e^- scattering cross section, $R(s) = \sigma(e^+e^- \to q\bar{q})/\sigma(e^+e^- \to \mu^+\mu^-)$. The experimentally observed cross section is proportional to the imaginary part of the vacuum polarization function $\mathrm{Im}\Pi(s)$, and one can use Cauchy's integral to extend the region of momentum squared q^2, which can be schematically written as

$$\Pi(q^2) = \frac{1}{\pi}\int_{s_0}^{\infty} ds \frac{\mathrm{Im}\Pi(s)}{s - q^2}. \tag{1}$$

(Strictly speaking, one needs to use the subtracted ones or derivatives to avoid divergences.) The q^2 of $\Pi(q^2)$ could be space-like (or Euclidean), for which a lattice calculation is applicable.

This strategy has indeed been used for the determination of $|V_{us}|$ through τ lepton decay [2]. Here, the decay rate has been measured as a function of the invariant mass of the final hadronic states (or the virtual W^* mass), and the lattice technique is used to calculate the left-hand side in the Euclidean momentum region. One can also consider the integral with multiple poles, so that the best sensitivity to $|V_{us}|$ is achieved while suppressing the systematic errors.

⋆ Speaker, e-mail: shoji.hashimoto@kek.jp

The region of q^2 may be extended from the space-like ($q^2 = -q_0^2 - \mathbf{q}^2$) region to the time-like ($q^2 = \omega^2 - \mathbf{q}^2$) region by applying the "Fourier transform" of the form

$$\Pi(q^2) = \int dt e^{-\omega t} \int d^3\mathbf{x} e^{i\mathbf{q}\cdot\mathbf{x}} \langle J^E(\mathbf{x}, t) J^E(\mathbf{0}, 0)\rangle \tag{2}$$

with an arbitrary (real) ω, until one hits any singularity. For the case of e^+e^- scattering, the condition is $\omega < m_V$ (or $\omega < 2m_\pi$ when the two-pion threshold opens). A demonstration of the method may be found in [3].

This work extends such analysis to the case of B meson decays, for which the initial state is a hadron. The kinematics is more complicated with two invariant kinematical variables $p \cdot q$ and q^2. Moreover, in the lattice calculation, we need to extract the ground state for the initial state while performing the Fourier transform to control the virtuality of the final states, which is the main challenge in this work.

A full description of the proposal and a pilot calculation is found in [4]. This contribution contains a development since then. Namely, the lattice data are updated with improved statistics and the comparison with the heavy quark expansion now includes one-loop corrections (see Section 4).

2 Semi-leptonic B decays

For the inclusive B decays there is a standard formalism [5–7] borrowed from the analysis of deep inelastic scattering.

Consider a B meson decay to a final state $X\ell\bar{\nu}_\ell$ with X an arbitrary state including a charm quark. The two leptons $\ell\bar{\nu}_\ell$ are generated from a virtual W and carry four-momentum q^μ so that the momentum transfer is q^2. The initial B meson has momentum $p_B^\mu = M_B v^\mu$, and the final hadrons have a total momentum p_X^μ. Since we consider the inclusive decays, the invariant mass $m_X^2 = p_X^2$ is arbitrary. It starts from the ground state D meson mass squared m_D^2, and more hadrons ($D\pi$, $D\pi\pi$, ...) are created as m_X^2 increases.

We are interested in the differential decay rate of the B meson, which is proportional to

$$|\mathcal{M}|^2 = |V_{qQ}|^2 G_F^2 M_B l^{\mu\nu} W_{\mu\nu}. \tag{3}$$

Other than the usual factors, the CKM matrix element $|V_{qQ}|$ and the Fermi constant G_F, the amplitude squared is written in terms of the known leptonic tensor $l^{\mu\nu}$ and the hadronic tensor $W_{\mu\nu}$, which needs to be non-perturbatively calculated. The hadronic tensor may be expressed as

$$W_{\mu\nu} = \sum_X (2\pi)^3 \delta^{(4)}(p_B - q - p_X) \frac{1}{2M_B} \langle B(p_B)|J_\mu^\dagger(0)|X\rangle\langle X|J_\nu(0)|B(p_B)\rangle \tag{4}$$

with all possible final states $|X\rangle$ inserted. The current J_μ has the $V - A$ structure $J_\mu = \bar{q}\Gamma_\mu Q$ with $\Gamma_\mu \equiv \gamma_\mu(1 - \gamma_5)$.

The hadronic tensor is a function of two Lorentz invariant variables $v \cdot q$ and q^2. Using the optical theorem, it is related to a forward scattering matrix element

$$T_{\mu\nu}(v \cdot q, q^2) = i \int d^4x e^{-iqx} \frac{1}{2M_B} \langle B(v)|T\left\{J_\mu^\dagger(x) J_\nu(0)\right\}|B(v)\rangle \tag{5}$$

as $-(1/\pi)\mathrm{Im}T = W$. The matrix element $T(v \cdot q, q^2)$ has an analytic structure shown in Figure 1. There is a physical cut related to W on the left, and the other cut on the right is an unphysical one corresponding to $\bar{c}bb$ final states.

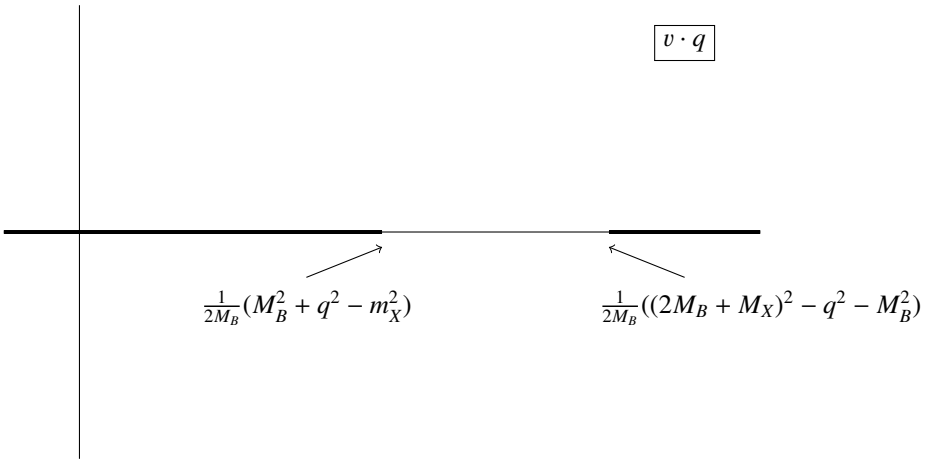

Figure 1. Analytic structure of the structure function $T(v \cdot q, q^2)$ in the complex plane of $v \cdot q$. The cuts are shown by thick lines. The cut on the left corresponds to the physical decay of $b \to c$, while the other represents an unphysical process $b \to \bar{c}bb$.

The strategy we propose in this work is to use Cauchy's integral

$$T(v \cdot q) = \frac{1}{\pi} \int_{-\infty}^{(v \cdot q)_{\max}} d(v \cdot q') \frac{\mathrm{Im} T(v \cdot q')}{v \cdot q' - v \cdot q} \tag{6}$$

to relate the physical amplitude on the right hand side to the matrix element at arbitrary $v \cdot q$, which may be an unphysical value. We take $v \cdot q$ above its maximum value allowed for the physical process $(v \cdot q)_{\max} = \frac{1}{2M_B}(M_B^2 + q^2 - m_X^2)$. There is no singularity around this $(v \cdot q)$, and the lattice calculation is applicable. Perturbative QCD is also considered to be more convergent away from the physical cut. We therefore propose to make a comparison in this unphysical kinematical region. In order to extract $|V_{cb}|$ or $|V_{ub}|$ from such an analysis, a reanalysis of the experimental data is necessary to perform the Cauchy integral.

3 Lattice calculation

We carry out a pilot lattice calculation of the matrix element $T_{\mu\nu}(v \cdot q, q^2)$. It amounts to calculate a four-point function shown in Figure 2. After taking appropriate ratios to cancel the external B meson smeared source, we construct

$$C_{\mu\nu}^{JJ}(t; \mathrm{q}) = \int d^3\mathbf{x} e^{i\mathbf{q}\cdot\mathbf{x}} \frac{1}{2M_B} \langle B(\mathbf{0}) | J_\mu^\dagger(\mathbf{x}, t) J_\nu(0) | B(\mathbf{0}) \rangle. \tag{7}$$

Here we take vanishing spatial momentum for the initial B meson and insert a momentum $\mathbf{q}$ $(-\mathbf{q})$ at the $b \to c$ current J_μ (or J_ν). We finally perform the "Fourier transform" in the time direction as

$$T_{\mu\nu}^{JJ}(\omega, \mathbf{q}) = \int_0^\infty dt e^{\omega t} C_{\mu\nu}^{JJ}(t; \mathbf{q}) \tag{8}$$

to obtain the matrix element at an unphysical kinematical point $p_X = (\omega, -\mathbf{q})$, $q = (M_B - \omega, \mathbf{q})$.

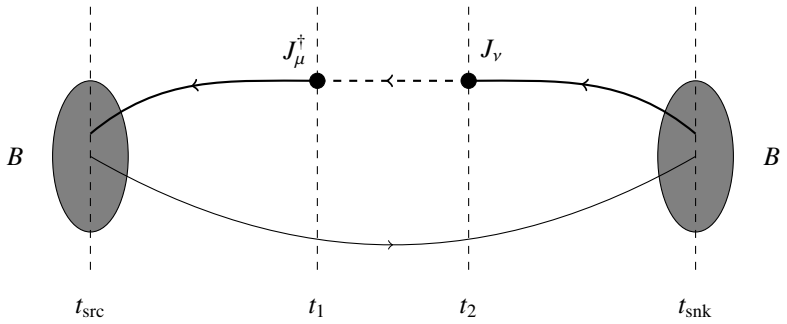

Figure 2. Four-point function to be calculated on the lattice to extract the matrix element $T_{\mu\nu}(v \cdot q, q^2)$. Valence quark lines are shown. Thick lines show the b quark line which decays to c quark drawn by a dashed line. The thin line represents a spectator quark.

We use the lattice ensembles generated with 2+1-flavors of dynamical quarks described by Möbius domain-wall fermion. The ensembles are generated at three lattice spacings a corresponding to $1/a =$ 2.4, 3.6, and 4.5 GeV. In order to keep the physical volume constant, the lattice size is scaled as $32^3 \times 64$, $48^3 \times 96$, and $64^3 \times 128$ for the different lattice spacings, respectively. Among four different values of light quark mass we take for simulation, we use the ensembles that have a pion mass 300 MeV. The same set of ensembles has been used for various calculations including a determination of charm quark mass [8], a calculation of D and B meson decay constants [9], as well as D meson decay form factors [10]. At this conference, an update of [10] is given by Kaneko [11], and a preliminary calculation of the $B \to \pi$ form factor is presented by Colquhoun [12]. We use the code set Iroiro++ for the numerical calculations [13].

The b quark mass we took is lower than the physical one, because of larger discretization effect for heavier quarks even on our fine lattice. The signal-to-noise ratio also sets a severe limit on the value of b quark mass one can set. We took $m_b = (1.25)^2 m_c$ as well as $(1.25)^4 m_c$.

Figure 3 shows the matrix element $C_{\mu\nu}^{JJ}(t; \mathbf{q})$ in the limit of zero recoil momentum $\mathbf{q} = \mathbf{0}$. It is plotted as a function of t_1 ($t = t_2 - t_1$ with a fixed t_2), and shows an exponential fall-off due to the propagation of final charm hadrons. At long distances, the correlation function is dominated by the ground state, which is D or D^* meson depending on the channel. The temporal channel $V_0 V_0$ (squares) is saturated by D, while the spatial channel $A_k A_k$ ($k = 1$, circles) is well described by D^*. The saturated exponential function is shown by dashed lines in the plot. At short distances, on the other hand, the correlation function contains a significant contribution from excited states including $D\pi$, $D\pi\pi$, ... etc., which can be seen as a departure from the dashed lines.

We then integrate $C_{\mu\nu}^{JJ}(t; \mathbf{q})$ over t according to (8). When $C_{\mu\nu}^{JJ}(t; \mathbf{q})$ is saturated by the ground state, $e^{-m_{D^{(*)}} t}$, the integral gives a pole $1/(m_{D^{(*)}} - \omega)$, which represents the propagator of the $D^{(*)}$ meson. Figure 4 shows the result of the integral as a function of $\omega = M_B - q_0$. The variable ω plays the role of the energy injected to the final charm hadron states. Since the correlation function $C_{\mu\nu}^{JJ}(t; \mathbf{q})$ is already close to the exponential function representing the ground state, the result also suggests the dominance of the ground state.

If we assume the ground state saturation, the correlation may be written in terms of the corresponding form factors. In the zero-recoil limit, they are defined by

$$\langle D(\mathbf{0})|V_0|B(\mathbf{0})\rangle = 2\sqrt{M_B M_D} h_+(1), \quad \langle D^*(\mathbf{0})|A_k|B(\mathbf{0})\rangle = 2\sqrt{M_B M_D} h_{A_1}(1)\varepsilon_k^*, \tag{9}$$

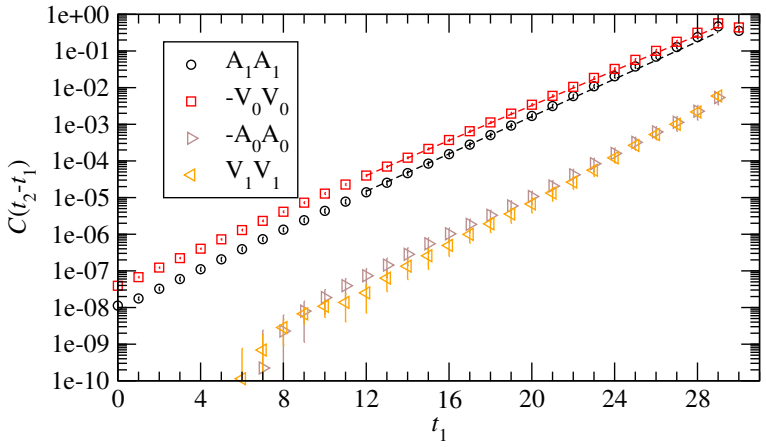

Figure 3. Correlation function $C^{JJ}_{\mu\nu}(t;\mathbf{q})$ plotted as a function of t_1. The other current t_2 is set at 30, and $t = t_2 - t_1$. Data for the AA channel in the spatial direction $\mu\nu = 11$ (circles) and for the VV channel in the temporal direction $\mu\nu = 00$ (squares) give the major contribution. Other channels (temporal AA and spatial VV) are an order of magnitude smaller. The dashed lines show the exponential decay due to the ground state D meson (red) and D^* meson (black). The data at $\beta = 4.35$ ($1/a \simeq 3.6$ GeV) and $m_b = (1.25)^4 m_c$ are shown.

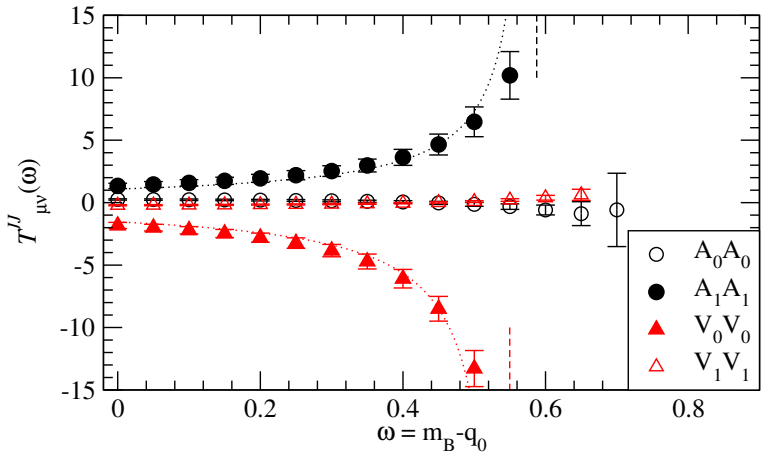

Figure 4. Structure functions $T^{JJ}_{\mu\nu}(\omega)$ for both $JJ = VV$ and AA channels. The lattice data are those of $\beta = 4.35$ ($1/a \simeq 3.6$ GeV). The values of ω can be taken continuously; here we take some representative ones for this plot. Both axes are in the lattice unit. Vertical dashed lines show the position of the nearby poles for the channels of spatial AA (red) and temporal VV (black). Dotted lines are estimated contributions of the ground state pole.

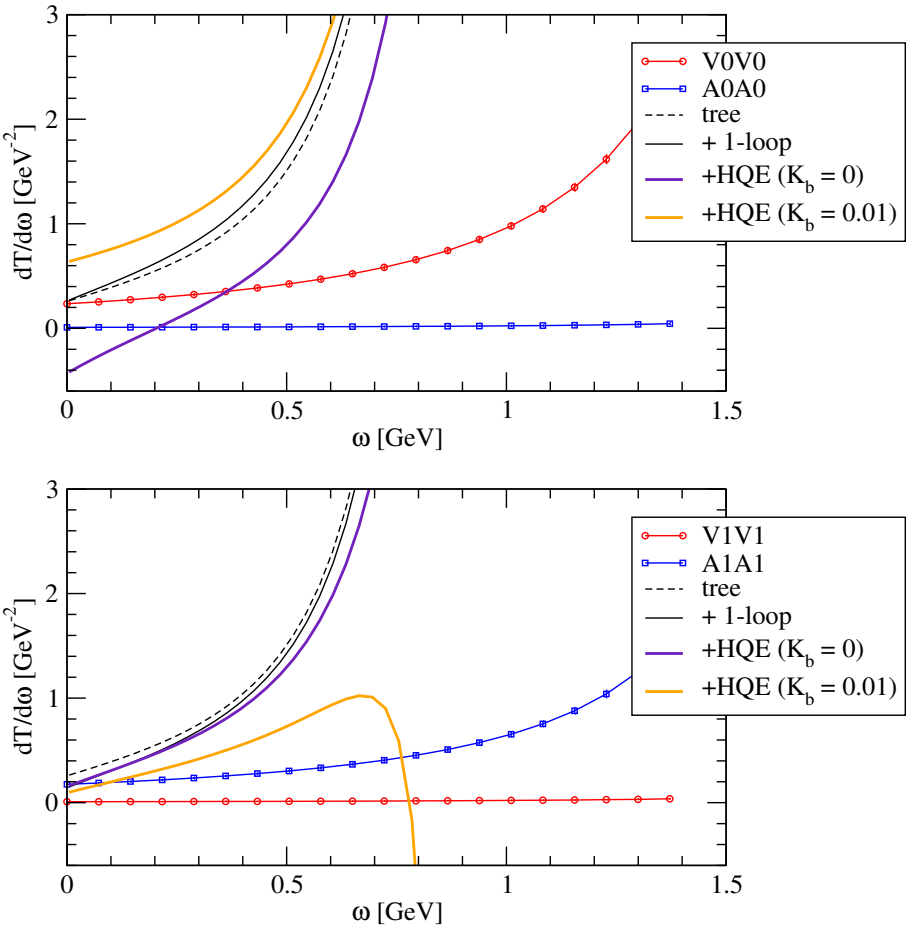

Figure 5. First derivative of $T_{\mu\nu}(\omega)$ with respect to ω. Temporal ($\mu = \nu = 0$) and spatial ($\mu\nu = k$) components are shown in the top and bottom panels, respectively. Lattice data are drawn with symbols: V_0V_0 (red) and A_kA_k (blue). Other curves are from the heavy quark expansion. See the text for the details.

and using them the structure functions are given as

$$T_{00}^{VV}(\omega, \mathbf{0}) = \frac{|h_+(1)|^2}{M_D - \omega}, \quad T_{kk}^{AA}(\omega, \mathbf{0}) = \frac{|h_{A_1}(1)|^2}{M_{D^*} - \omega}. \tag{10}$$

The zero-recoil form factors $h_+(1)$ and $h_{A_1}(1)$ is normalized to unity in the heavy quark limit. The correction due to finite m_b and m_c makes them smaller than 1, and our results are roughly consistent with the known values [14] as well as with the mass dependence studied in [15, 16].

4 Comparison with heavy quark expansion

We consider a first derivative $dT_{\mu\nu}^{JJ}/d\omega$ instead of $T_{\mu\nu}^{JJ}$ themselves to avoid possible divergences due to a contact term contribution. Figure 5 shows this quantity as a function ω. The spatial momentum

insertion **q** is fixed to zero. The lattice data may be obtained by calculating a t moment analogous to (8). On the lattice we separately calculate V_0V_0 (red) and A_kA_k (blue), while the results from heavy quark expansion are plotted only for the combination $VV + AA$, which corresponds to the product of the $V - A$ currents. For the comparison, we can neglect the one (AA or VV) depending on the channel as the lattice results indicate.

The continuum estimate using perturbative QCD and the heavy quark expansion is expected to be valid away from the resonance region. In terms of the injected energy to the final hadron ω, the small ω region is perturbative.

In the plot, the estimates from the heavy quark expansion are shown by dashed and solid curves. The dashed curve is the leading order estimate for both α_s and $1/m_b$. The one-loop correction is included for the solid black curve, which is obtained from the one-loop calculation of the differential decay rate [17, 18] by doing the Cauchy integral. The result suggests that the perturbative series is sufficiently convergent.

The $1/m_b$ correction consists of two terms, each involving the hadronic matrix elements

$$\mu_G^2 = \frac{1}{2M_B}\langle B|\bar{Q}\frac{i}{2}\sigma_{\mu\nu}G^{\mu\nu}Q|B\rangle, \tag{11}$$

$$\mu_\pi^2 = \frac{1}{2M_B}\langle B|\bar{Q}(i\vec{D})^2Q|B\rangle. \tag{12}$$

The former is well determined, $\simeq 0.37$ GeV^2, by the experimentally measured $B - B^*$ mass splitting, while the latter is more uncertain and only an order of magnitude estimate, ~ 0.5 GeV^2, is available.

The estimates at the order of $1/m_b$ are shown by thick curves for $\mu_\pi^2 = 0$ (purple) and 0.5 GeV^2 (orange). It turned out that the size of the $1/m_b$ correction is substantial, and the uncertainty due to unknown μ_π^2 is large.

Rough agreement between the lattice results and the heavy quark expansion estimates is found near $\omega \approx 0$. The slope at $\omega = 0$, however, is much larger with the continuum estimates. This seems to be unavoidable because the continuum formula contains a pole at $m_c \simeq 1$ GeV, which is much lower than the actual hadronic poles at $m_{D^{(*)}} \sim 2$ GeV. It is probable that this problem may be avoided by rearranging the perturbative series such that the fake pole of the bare quark is eliminated.

5 Outlook

The structure functions for the inclusive B meson decay are calculable on the lattice but at unphysical kinematical points, which can be related to the observed differential decay rate by Cauchy's integral. In this talk we presented a pilot study for the $b \to c$ transition with the b quark mass still lower than the physical one. The lattice results are compared with the predictions of perturbative QCD and the heavy quark expansion.

The range of application of this method is not limited to the inclusive $b \to c$ transitions. An interesting application is the test of the zero-recoil sum rule, which is used to estimate the zero-recoil $B \to D^{(*)}\ell\nu$ form factor [19–22]. Another obvious application is the $b \to u$ transition and the determination of $|V_{ub}|$.

Since the formalism of the structure function comes from the nucleon deep inelastic scattering, the method developed in this work may be applied to the study of nucleon structure. The unphysical kinematical region considered in this work corresponds to the value of Bjorken x greater than 1, which can be reached by the Cauchy integral of the physical region $0 < x < 1$. A study along this direction is initiated by [23]. It provides a new method to constrain the parton distribution functions. Since the lattice calculation is fully non-perturbative, the ep (or νp) scattering at relatively low-energies can be studied.

Acknowledgments

We thank the members of the JLQCD collaboration for discussions and for providing the computational framework and lattice data. Numerical calculations are performed on Blue Gene/Q at KEK under its Large Scale Simulation Program (No. 16/17-14), on Oakforest-PACS supercomputer operated by Joint Center for Advanced High Performance Computing (JCAHPC). This work is supported in part by JSPS KAKENHI Grant Number JP26247043 and by the Post-K supercomputer project through the Joint Institute for Computational Fundamental Science (JICFuS).

References

[1] J. Dingfelder, T. Mannel, Rev. Mod. Phys. **88**, 035008 (2016)
[2] K. Maltman, R.J. Hudspith, R. Lewis, T. Izubuchi, H. Ohki, J.M. Zanotti, Mod. Phys. Lett. **A31**, 1630030 (2016)
[3] X. Feng, S. Hashimoto, G. Hotzel, K. Jansen, M. Petschlies, D.B. Renner, Phys. Rev. **D88**, 034505 (2013), 1305.5878
[4] S. Hashimoto, PTEP **2017**, 053B03 (2017), 1703.01881
[5] J. Chay, H. Georgi, B. Grinstein, Phys. Lett. **B247**, 399 (1990)
[6] A.V. Manohar, M.B. Wise, Phys. Rev. **D49**, 1310 (1994), hep-ph/9308246
[7] B. Blok, L. Koyrakh, M.A. Shifman, A.I. Vainshtein, Phys. Rev. **D49**, 3356 (1994), [Erratum: Phys. Rev.D50,3572(1994)], hep-ph/9307247
[8] K. Nakayama, B. Fahy, S. Hashimoto, Phys. Rev. **D94**, 054507 (2016), 1606.01002
[9] B. Fahy, G. Cossu, S. Hashimoto, PoS **LATTICE2016**, 118 (2016), 1702.02303
[10] T. Kaneko, B. Fahy, H. Fukaya, S. Hashimoto (JLQCD), PoS **LATTICE2016**, 297 (2017), 1701.00942
[11] T. Kaneko, B. Colquhoun, H. Fukaya, S. Hashimoto (JLQCD), *D meson semileptonic form factors in Nf=3 QCD with Möbius domain-wall quarks* (2017), 1711.11235
[12] B. Colquhoun, S. Hashimoto, T. Kaneko, *$B \to \pi \ell \nu$ with Möbius Domain Wall Fermions* (2017), 1710.07094
[13] G. Cossu, J. Noaki, S. Hashimoto, T. Kaneko, H. Fukaya, P.A. Boyle, J. Doi, *JLQCD IroIro++ lattice code on BG/Q* (2013), 1311.0084
[14] J.A. Bailey et al. (MILC), Phys. Rev. **D92**, 034506 (2015), 1503.07237
[15] S. Hashimoto, A.X. El-Khadra, A.S. Kronfeld, P.B. Mackenzie, S.M. Ryan, J.N. Simone, Phys. Rev. **D61**, 014502 (1999), hep-ph/9906376
[16] S. Hashimoto, A.S. Kronfeld, P.B. Mackenzie, S.M. Ryan, J.N. Simone, Phys. Rev. **D66**, 014503 (2002), hep-ph/0110253
[17] M. Trott, Phys. Rev. **D70**, 073003 (2004), hep-ph/0402120
[18] V. Aquila, P. Gambino, G. Ridolfi, N. Uraltsev, Nucl. Phys. **B719**, 77 (2005), hep-ph/0503083
[19] M.A. Shifman, N.G. Uraltsev, A.I. Vainshtein, Phys. Rev. **D51**, 2217 (1995), [Erratum: Phys. Rev.D52,3149(1995)], hep-ph/9405207
[20] I.I.Y. Bigi, M.A. Shifman, N.G. Uraltsev, A.I. Vainshtein, Phys. Rev. **D52**, 196 (1995), hep-ph/9405410
[21] A. Kapustin, Z. Ligeti, M.B. Wise, B. Grinstein, Phys. Lett. **B375**, 327 (1996), hep-ph/9602262
[22] P. Gambino, T. Mannel, N. Uraltsev, JHEP **10**, 169 (2012), 1206.2296
[23] A.J. Chambers, R. Horsley, Y. Nakamura, H. Perlt, P.E.L. Rakow, G. Schierholz, A. Schiller, K. Somfleth, R.D. Young, J.M. Zanotti, Phys. Rev. Lett. **118**, 242001 (2017), 1703.01153